



The role of Pd–Ga bimetallic particles in the bifunctional mechanism of selective methanol synthesis via CO₂ hydrogenation on a Pd/Ga₂O₃ catalyst

Sebastián E. Collins^{a,*}, Juan J. Delgado^b, César Mira^b, José J. Calvino^b, Serafín Bernal^b, Dante L. Chiavassa^a, Miguel A. Baltanás^a, Adrian L. Bonivardi^a

^a Instituto de Desarrollo Tecnológico para la Industria Química, Universidad Nacional del Litoral and CONICET, Güemes 3450, 3000 Santa Fe, Argentina

^b Dpto. de Ciencias de los Materiales, Ingeniería Metalúrgica y Química Inorgánica, Facultad de Ciencias, Universidad de Cádiz, Puerto Real E11510, Spain

ARTICLE INFO

Article history:

Received 24 April 2012

Accepted 2 May 2012

Available online 15 June 2012

Keywords:

Palladium

Gallium

Bimetallic

Methanol synthesis

HRTEM

Infrared spectroscopy

ABSTRACT

The effect of palladium–gallia interaction in Pd(1 wt.)/β-Ga₂O₃ during selective methanol synthesis by CO₂ hydrogenation was studied. A detailed quasi-in situ transmission electron microscopy analysis of the as-prepared H₂-reduced catalyst, without exposing it to air, showed that Ga–Pd bimetallic (nano)particles were formed under a reductive atmosphere at or above 523 K. However, these particles were unstable; upon air exposure, a dramatic and extensive encapsulation of the metallic crystallites by Ga₂O₃ occurred. In addition, the function of the bimetallic particles in the mechanism of methanol synthesis was investigated by in situ infrared spectroscopy at 0.7 MPa. The results confirmed those of previous studies in which the stepwise hydrogenation of (bi)carbonate to formate and then to methoxy groups on the Ga₂O₃ surface took place via a bifunctional pathway. In this pathway, the role of the Ga–Pd bimetallic crystallites was to provide atomic hydrogen, via spillover, to the oxidic surface and to hamper both CH₃OH decomposition and CO production.

© 2012 Elsevier Inc. All rights reserved.

1. Introduction

Methanol synthesis from CO₂/H₂ is a viable alternative for reducing greenhouse gas net emissions. In this context, supported precious metals, such as palladium, have been of particular interest over the past decade [1], as it is well known that both the support and the (eventual use of a) promoter can appreciably modify the activity and/or selectivity of this metal in methanol synthesis [2–4].

The development of an active Pd/Ga₂O₃ catalyst for selective methanol synthesis from CO₂ hydrogenation able to compete with the classical Cu/ZnO formulation was first reported by Fujitani et al. [4]. Using a stoichiometric H₂/CO₂ mixture (523 K, 5 MPa), their Pd/Ga₂O₃ preparations were 120-fold more active than Pd on SiO₂ (an inert support) and sevenfold more active than Cu/ZnO/Al₂O₃ [4,5]. It was suggested that the other reaction product, CO, was obtained (with selectivity close to 49%) via the reverse water–gas shift reaction (RWGS) over the metallic particles.

A sustained research effort has been conducted by some of us during the past decade to understand the origin of the remarkable performance of the palladium–gallia system for the selective hydrogenation of CO₂ to methanol. First, Bonivardi et al. [6] showed that gallium oxide addition (as a promoter) to a Pd (2 wt.)/SiO₂ catalyst increased the CH₃OH production rate in the

hydrogenation of carbon dioxide at conventional process conditions up to 500-fold (523 K, 3 MPa, H₂/CO₂ = 3) compared to Pd/SiO₂. At the same time, methanol selectivity was enhanced up to 70%, compared to a meager 10% in the unpromoted catalyst.

Later, detailed studies on the chemical structure and reaction mechanisms were undertaken. The interaction of H₂ with Ga₂O₃/SiO₂, Pd/SiO₂, Ga₂O₃–Pd/SiO₂, and pure Ga₂O₃ polymorphs with different crystallographic phases (α,β,γ) was investigated by in situ X-ray photoelectron and Fourier transform infrared spectroscopy (XPS and FTIR, respectively) [7,8]. The adsorption of CO₂ over this set of gallium oxide polymorphs was also examined via infrared spectroscopy. Two types of bicarbonate species (mono- and bidentate), carboxylate, bridge carbonate, bidentate carbonate, and polydentate carbonate species were identified [9]. Interestingly, most of these carbonates were reversibly adsorbed on the gallia surface.

A detailed study of CO₂ hydrogenation to methanol, as well as of methanol decomposition, on model Pd/gallia catalysts was likewise conducted, mainly by means of in situ FTIR [10,11]. It was shown that the reaction intermediates, chemisorbed onto gallia, were successively hydrogenated from (bi)carbonates to formate (mono- and bidentate and bridged), methylenebisoxo, and methoxy to give methanol, while hydrogen supply was accomplished via *spillover* from the palladium metal particles. The same intermediates were identified during methanol decomposition (i.e., the reverse pathway) on pure Ga₂O₃ polymorphs and Pd/Ga₂O₃ catalysts

* Corresponding author. Fax: +54 342 4550944.

E-mail address: scollins@santafe-conicet.gov.ar (S.E. Collins).

[11,12]. Further work using physical mixtures of $\text{Ga}_2\text{O}_3/\text{SiO}_2$ and Pd/SiO_2 showed that atomic hydrogen, H_s , was generated on the silica-supported Pd particles and moved (“spilled over”) to the supported gallia particles, where the carbonaceous species were then hydrogenated [13]. These reaction results indicated that (as was also evidenced by in situ FTIR) the $\text{Ga}_2\text{O}_3\text{-Pd}/\text{SiO}_2$ catalyst worked as a true bifunctional system, while Pd/SiO_2 did not.

The collected spectroscopic information was successfully used to develop a comprehensive microkinetic model that was able to account for the reaction performance of the gallia-promoted Pd catalyst for the selective synthesis of methanol from CO_2/H_2 (together with the undesirable RWGS reaction) under a wide range of operating conditions [14].

Notwithstanding, some authors have postulated that Pd–Ga alloys may play a relevant role in the catalytic activity of the palladium–gallia systems. Iwasa and coworkers [15,16], for example, were the first to suggest that the remarkable activity and selectivity achieved by $\text{Pd}/\text{Ga}_2\text{O}_3$ catalysts, either in methanol synthesis or in the steam reformation of methanol, was a consequence of the new metallic catalytic function performed by a Pd–Ga alloy. Later, a series of pure Pd–Ga intermetallic compounds showing high activity and selectivity in the hydrogenation of acetylene in an ethylene-rich stream were prepared by Schlögl and coworkers [17–19]. Very recently, $\text{Pd}/\text{Ga}_2\text{O}_3$ catalysts have been investigated in the methanol–steam reformation reaction using different oxidative and reductive pretreatments [20–22]. The authors reported the formation of Pd–Ga bimetallic particles during reductive pretreatment above 523 K. In agreement with the work of Iwasa and coworkers [15,16], the Pd–Ga bimetallic particles were claimed to be the sites responsible for the increased selectivity to CO_2 over methanol decomposition to CO and H_2 . Likewise, the possibility of the formation of a Pd–Ga alloy on $\text{Pd}/\text{Ga}_2\text{O}_3$ catalysts under methanol synthesis conditions was suggested a few years ago [23], but its relevance in the catalytic performance of this system in the CO_2 hydrogenation remained unclear. Therefore, we present here an investigation of a $\text{Pd}/\beta\text{-Ga}_2\text{O}_3$ model catalyst to gain further insight into the role(s) of any possible alloy formation and its impact on the catalytic performance of this material in H_2/CO_2 mixtures. Reaction performance, in situ characterization, and high-pressure IR spectroscopy were combined to compare the possible (or eventual) influence of the bimetallic Pd–Ga in the bifunctional mechanism of methanol synthesis from CO_2 hydrogenation.

2. Experimental

2.1. Catalyst

$\text{Pd}(1 \text{ wt.}\%)/\beta\text{-Ga}_2\text{O}_3$ was prepared by incipient wetness impregnation using $\text{Pd}(\text{OAc})_2$ (Sigma) in acetone, with further drying/calcination in air (673 K, 2 h), H_2 reduction (2% H_2/Ar , 723 K, 2 h), and passivation with oxygen pulses at room temperature. This material is named “as-prepared” or “pre-reaction” $\text{Pd}/\text{Ga}_2\text{O}_3$. The monoclinic $\beta\text{-Ga}_2\text{O}_3$ was obtained by calcining gallia (Strem, 99.998%) at 1073 K for 5 h. CO pulses were used to determine the palladium dispersion ($D_{\text{CO}} = 31\%$) on the as-prepared catalyst, which was re-reduced at 523 K (pure H_2 , 1 h) using a conventional technique [24]. The BET (N_2) areas of the support and the catalyst were both $12 \text{ m}^2 \text{ g}^{-1}$. Pd (1 wt.%) / SiO_2 was prepared and characterized as described previously [6].

2.2. Catalytic activity tests

The catalytic performance was evaluated in a differential plug-flow reactor [$\text{H}_2/\text{CO}_2 = 3$, 523 K, 0.7 MPa ($\text{SV} = 7700 \text{ h}^{-1}$) and 3 MPa ($\text{SV} = 80,000 \text{ h}^{-1}$)] over 24 h. Each catalyst was re-reduced inside

the reactor by flowing H_2 (heating rate 3 K min^{-1} , $P = 0.1 \text{ MPa}$) from RT to 523 K and maintaining the hydrogen flow for 1 h. Gas chromatography was used to analyze the gas composition in two Shimadzu 9A units arranged in parallel that employed Porapak QS and Carbosieve SII-filled (1/8 in. ID, 3 m long) stainless steel columns with TCD and FID, respectively.

After the reaction test, the reactor was depressurized, the feed of reactants was replaced by pure H_2 ($60 \text{ cm}^3 \text{ min}^{-1}$, at 523 K), and the unit was allowed to cool to room temperature under this flow. Then the reactor was swept with pure N_2 (99.999%, $60 \text{ cm}^3 \text{ min}^{-1}$), and oxygen pulses were gradually introduced into the gas stream to passivate the catalyst before its exposure to air and final storage in a desiccator. This sample is referred to hereafter as “postreaction $\text{Pd}/\text{Ga}_2\text{O}_3$.”

2.3. High-resolution electron microscopy

High-resolution transmission (HRTEM) and high-angle annular dark-field scanning–transmission (HAADF-STEM) micrographs were obtained using a JEOL-2010F microscope equipped with a field emission gun and operated at an acceleration voltage of 200 kV. The structural resolution of the equipment in the HRTEM mode was 0.19 nm at the Scherzer defocus conditions, while the diameter of the probe used in STEM was 0.5 nm. The intensity of the HAADF-STEM images is proportional (sensitive) to the square of the atomic number. Due to this proportionality, we can unambiguously discriminate between Pd ($Z = 46$) and the cation of the support, Ga ($Z = 31$), for accurate determination of the average size distribution of the metal particles.

Taking advantage of the STEM mode, elemental analysis studies were performed at the nanometric scale by X-ray energy-dispersive spectroscopy (X-EDS), using an Oxford INCA Energy 2000 system coupled to the equipment. The chemical composition of the supported nanoparticles was studied using both spot and line spectrum measurements. The latter approach was useful for determining the distribution of Pd and Ga. The sample was mounted on a copper grid by a dry method to prevent the sample from coming into contact with any solvent.

2.4. Quasi-in situ transmission electron microscopy

A homemade quasi-in situ TEM system was used to evaluate the formation of bimetallic nanoparticles in the catalyst without exposure to the atmosphere. This setup featured a VTST4006 (GATAN Inc.) high-resolution vacuum transfer holder. The tip of this holder can be placed on a special quartz reactor to conduct thermochemical treatments, after which the sample is introduced into a shuttle chamber, under high vacuum, to place it inside the microscope under anaerobic conditions. This approach allows observation of samples without any further modification or degradation. The samples were deposited onto a lacey carbon-coated molybdenum grid, which was previously pretreated at 523 K under a H_2 atmosphere to prevent any contamination during the experiments.

2.5. Infrared studies

In situ transmission infrared spectroscopy was performed using $\approx 23 \text{ mg cm}^{-2}$ samples pressed into self-supported wafers at 5 ton cm^{-2} . The wafers were located in a heated Pyrex cell with water-cooled NaCl windows, which was attached to a conventional high-vacuum system (base pressure = $1.33 \times 10^{-4} \text{ Pa}$) and a manifold for gas flow. Infrared transmission spectra were acquired with a Nicolet Magna 550 Series II FTIR spectrometer using an MCT-A detector (resolution 4 cm^{-1} , 100 scans). Further processing of the spectra was carried out with Microcal Origin 4.1 software.

Background correction of the spectra was achieved by subtracting the spectra of the clean wafers after the activation pretreatment.

In situ reaction experiments, at high and low pressure, were performed in a homemade stainless steel transmission cell fitted with CaF_2 windows. The temperature was controlled by two thermocouples, one in the heating block and the other inserted inside the cell space and in contact with the catalyst wafer. High-pressure experiments were carried out by submitting the catalyst wafer to in situ reduction in pure H_2 from RT to 523 K (0.1 MPa , 5 K min^{-1} , $100 \text{ cm}^3 \text{ min}^{-1}$). Then the flow was changed to a stoichiometric $\text{H}_2/\text{CO}_2 = 1/3$ mixture, and the cell was pressurized to 0.7 MPa using a backpressure regulator. Transmission spectra were acquired and processed as described before.

3. Results

3.1. Characterization and catalytic activity

Table 1 summarizes the results of the morphological characterization, activity, and selectivity at steady state of the $\text{Pd}(1 \text{ wt.}\%)/\beta\text{-Ga}_2\text{O}_3$ catalyst activated under pure H_2 at 523 K for 60 min (hereafter as-prepared + R523/1 h). The results of the hydrogenation of CO_2 ($\text{H}_2/\text{CO}_2 = 3$, 523 K) over 24 h on stream, both at 3 MPa and at 0.7 MPa, are presented to compare the latter with in situ FTIR experiments. For comparison purposes, a $\text{Pd}(2 \text{ wt.}\%)/\text{SiO}_2$ reference catalyst subjected to the same pretreatment protocol is also included. Pure gallia was unreactive under these reaction conditions.

The specific rate of CO_2 hydrogenation to methanol was approximately 20-fold higher on the $\text{Pd}/\beta\text{-Ga}_2\text{O}_3$ catalyst than on the reference Pd/SiO_2 catalyst, or approximately 40-fold higher per metal site, based on their respective initial Pd dispersion. In addition, the former was fourfold more selective to methanol. The temporal evolution of the production rates of methanol and CO during 24 h of reaction on both catalysts is shown in Fig. 1. As observed, the activity at the beginning of the reaction over $\text{Pd}/\text{Ga}_2\text{O}_3$ was much higher toward the production of CO, but then decreased significantly. Meanwhile, the reverse was observed for the activity toward methanol. After approximately 3 h, the system reached a pseudo-steady state, with similar activity (and selectivity) for the production of methanol and CO. On the reference Pd/SiO_2 catalyst, only a moderate decrease in the rates to methanol and CO during the first hour of reaction was observed. On this catalyst, the selectivity to CO was also consistently and noticeably higher.

These progressive (and opposite) changes in activity toward methanol and CO on the $\text{Pd}-\text{Ga}_2\text{O}_3$ catalyst during the first 3 h of reaction prompted us to investigate this phenomenon further. Therefore, we set out to characterize the catalyst both before (pre) and after (post) the reaction, using TEM and FTIR in situ.

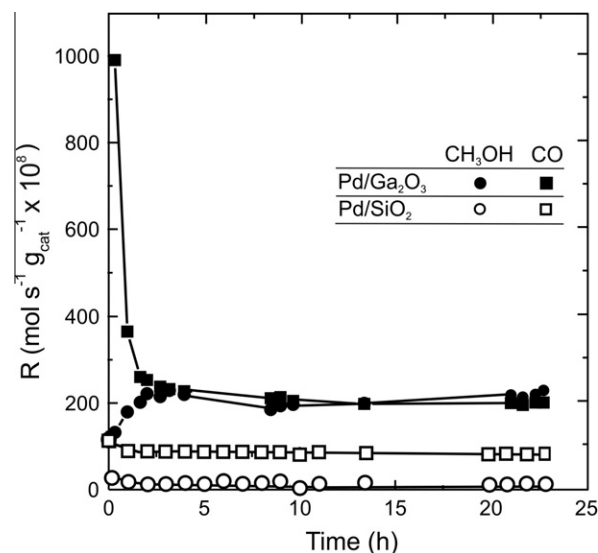


Fig. 1. Time evolution of the production rates of methanol and CO over the $\text{Pd}(1 \text{ wt.}\%)/\beta\text{-Ga}_2\text{O}_3$ catalyst as-prepared + R523/1 h and the reference $\text{Pd}(2 \text{ wt.}\%)/\text{SiO}_2$ catalyst ($\text{H}_2/\text{CO}_2 = 3$, $P = 3 \text{ MPa}$, $T = 523 \text{ K}$).

3.2. Nanostructural and nanoanalytical analyses by transmission electron microscopy

Fig. 2a and b shows a representative ex situ HRTEM image of the as-prepared $\text{Pd}/\text{Ga}_2\text{O}_3$ catalyst and its Pd particle size histogram, respectively. The structural parameters measured on the support indicated that the interplanar spaces and angles correspond to the monoclinic structure of $\beta\text{-Ga}_2\text{O}_3$. The Pd crystallites were uniformly distributed on the surface of the sample. As shown in Fig. 2b, the catalyst has a rather wide size distribution for the metal particles, with most between 1 and 3.5 nm ($d_p = 2.1 \text{ nm}$, $D_{\text{TEM}} = 41\%$). It was also noteworthy that the Pd crystallites appeared, in general, to be free of decoration, although some nanoparticles looked as if they were covered by a thin layer of an amorphous nature. Although this decoration was not statistically measurable, it might well be an indication of some alloy formation during the activation protocol, as will be discussed later.

The nanostructural morphology and chemical composition of the supported particles of the activated catalysis prior to the reaction (i.e., the as-prepared catalyst re-reduced at 523 K) were investigated by quasi-in situ TEM analysis. An aliquot of the as-prepared $\text{Pd}/\text{Ga}_2\text{O}_3$ stock was placed in a Mo grid and submitted to a reduction pretreatment in pure H_2 ($60 \text{ cm}^3 \text{ min}^{-1}$, 523 K, 6 h) inside a quartz microreactor (hereafter, as-prepared + R523). After reduction, the microreactor was evacuated ($P < 10^{-6} \text{ mbar}$) for 60 min

Table 1
Catalytic performance of the catalysts for CO_2 hydrogenation under pseudo-steady-state conditions.

| Catalysts and support ^a | $D_{\text{TEM}}^b(\%)$ | $D_{\text{CO}}^c(\%)$ | $S(\text{BET})(\text{m}^2 \text{g}^{-1})$ | Reaction pressure (MPa) | Activity ^d ($\text{mol g}^{-1} \text{s}^{-1}) \times 10^8$ | | | TOF ^e ($\text{s}^{-1}) \times 10^3$ | | Selectivity (%) | | |
|--|------------------------|-----------------------|---|-------------------------|--|-----|------------------|---|-----|--------------------|----|------------------|
| | | | | | CH ₃ OH | CO | DME ^f | CH ₃ OH | CO | CH ₃ OH | CO | DME ^d |
| $\text{Pd}(1 \text{ wt.}\%)/\beta\text{-Ga}_2\text{O}_3$ | 41 | 31 | 12 | 3 | 220 | 201 | 0 | 75 | 69 | 52 | 48 | 0 |
| | | | | 0.7 | 102 | 220 | 0 | 35 | 75 | 32 | 68 | 0 |
| $\beta\text{-Ga}_2\text{O}_3$ | – | – | 12 | 3 | 0 | 0 | Traces | – | – | 0 | 0 | – |
| $\text{Pd}(2 \text{ wt.}\%)/\text{SiO}_2$ | 58 | 56 | 265 | 3 | 11 | 85 | 0 | 2 | 9.5 | 12 | 88 | – |

^a Activation pretreatment of the as-prepared catalysts in flowing H_2 (heating rate, 3 K min^{-1} ; $P = 0.1 \text{ MPa}$) from RT to 523 K, maintaining the hydrogen flow for 1 h.

^b Metal dispersion of the as-prepared catalysts measured by TEM.

^c Metal dispersion of the as-prepared catalysts reduced at 523 K with pure H_2 (1 h) measured by CO pulses at RT [24].

^d After 20 h of reaction in a differential plug-flow microreactor (pseudo-steady-state conditions): $\text{H}_2/\text{CO}_2 = 3$, $T = 523 \text{ K}$, $\text{SV} = 80,000 \text{ h}^{-1}$ (3 MPa), $\text{SV} = 7700$ (0.7 MPa), CO_2 conversion $< 1\%$.

^e TOF: Turnover frequency, calculated as follows: $\text{TOF}_i(\text{s}^{-1}) = i\text{th product flow rate}(\text{mol g}^{-1} \text{s}^{-1})/\text{quantity of metal surface sites}(\text{mol g}^{-1})$; [i: CH_3O or CO]. Quantity of metal surface sites (mol g^{-1}) = $D_{\text{CO}} \times \text{metal loading}(\text{mol g}^{-1})$.

^f DME: Dimethyl ether.

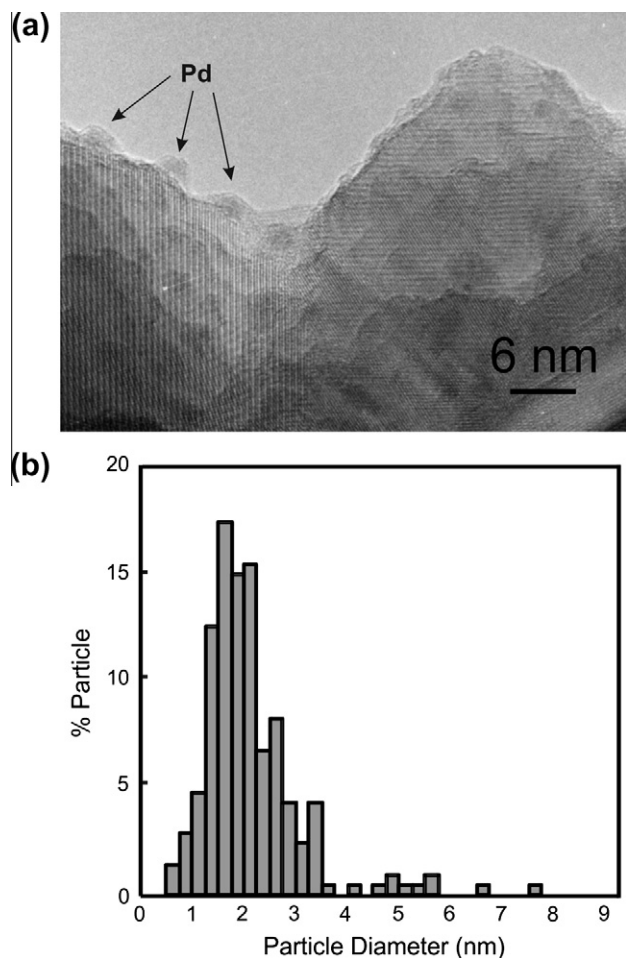


Fig. 2. HRTEM image of the prereaction Pd/ β -Ga₂O₃ catalyst (a) and metal particle size distribution (b).

and cooled under vacuum to RT. Next, the grid was transferred to the microscope without exposure of the sample to air.

Fig. 3a shows an illustrative HAADF-STEM image obtained after the reduction pretreatment. This HAADF-STEM image gave results similar to those for the as-prepared prereaction catalyst: Pd nanoparticles were homogeneously distributed on the support. A slight increase in particle size distribution was detected, though without a pronounced change in the overall particle shape. The metal crystallites appeared to be free of decoration.

Metal particles located on convex surfaces of the support were selected for chemical analysis by X-EDS. In particular, line-spectrum measurements were carried out through these particles along the lines traced in the figure. The intensity profiles of Pd and Ga in two of these particles are shown in Fig. 3b and c, respectively. The results clearly showed that gallium had been incorporated into the initial Pd nanoparticles during the reducing pretreatment. The X-EDS analysis was carried out across 20 particles, and reproducible results were obtained.

A representative high-resolution image of a metallic particle observed on the Pd/Ga₂O₃ catalyst after its exposure to pure H₂ at 523 K is included in Fig. 4. To identify the possible formation of Pd–Ga bimetallic particles, a digital diffraction pattern analysis of the HRTEM images was performed. The plane distances and angles observed were in good agreement with Pd₂Ga₅ in the [011] axis zone [25]. However, the small differences between this phase and the pure metallic Pd phase made it impossible to make unambiguous phase identification. Penner et al. previously reported that the Pd₅Ga₂, Pd₅Ga₃, and Pd₂Ga bimetallic phases exhibit

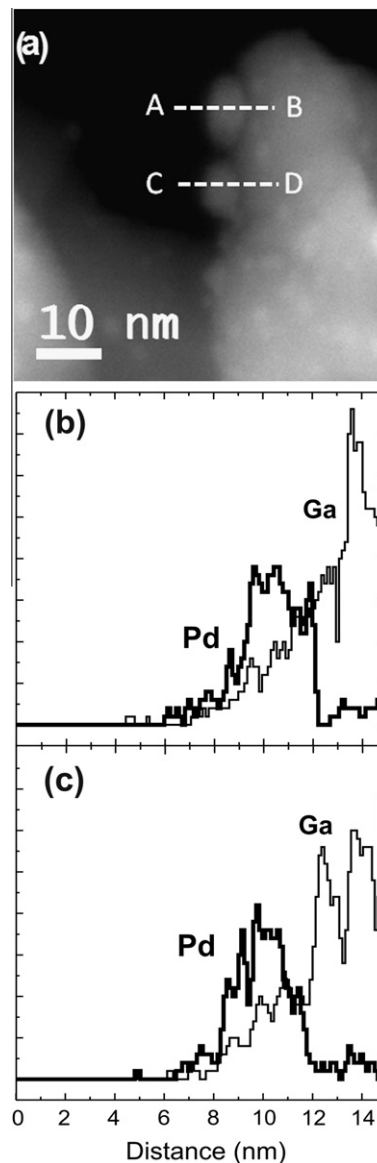


Fig. 3. (a) STEM-HAADF image of the Pd/Ga₂O₃ catalyst reduced quasi-in situ in pure H₂ at 523 K. (b and c) X-EDS line spectra through the A–B and C–D trajectories over selected metal particles (thin line, Ga; thick line, Pd; spatial resolution, 0.5 nm).

orthorhombic structures with similar lattice parameters (Pd₅Ga₃: $a = 5.50 \text{ \AA}$, $b = 10.53 \text{ \AA}$, $c = 4.40 \text{ \AA}$; Pd₅Ga₂: $a = 18.37 \text{ \AA}$, $b = 5.48 \text{ \AA}$, $c = 4.08 \text{ \AA}$; Pd₂Ga: $a = 5.46 \text{ \AA}$, $b = 4.03 \text{ \AA}$, $c = 7.81 \text{ \AA}$), giving rise to very similar diffraction patterns [20]. Thus, the close structural relationship between these Pd–Ga phases precluded a definitive assignment of a given bimetallic crystalline phase, as did the small crystal size of the particles in the sample and the intrinsic experimental error of the measurements. Nevertheless, the joint TEM and CO adsorption results (shown in the next section) of the Pd/Ga₂O₃ catalyst reduced with hydrogen at 523 K allowed us to conclude that bimetallic particles were formed on the surface of the gallia support upon hydrogen reduction.

To assess the stability of these Pd–Ga bimetallic particles, a complementary experiment was performed, in which the reduced catalyst sample was exposed to air at RT for 24 h and again placed in the microscope. The HRTEM and STEM-HAADF images confirmed that several particles became covered by a thin layer of Ga₂O₃ of an amorphous nature. Additionally, after 24 h on stream and air passivation at room temperature, the Pd/Ga₂O₃ catalyst was examined

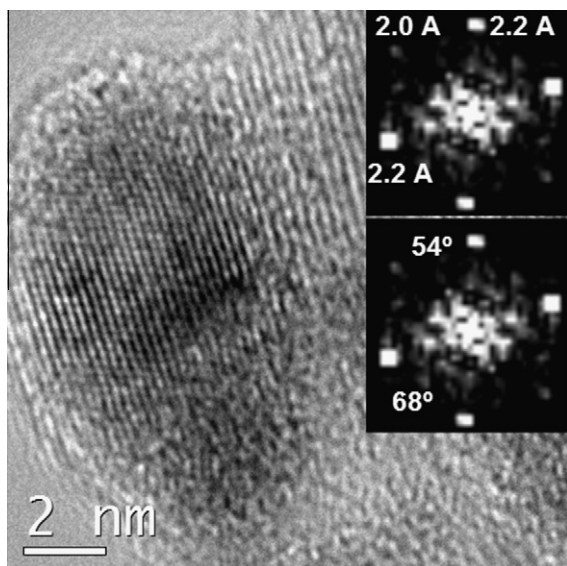


Fig. 4. DDP analysis of a representative Pd–Ga particle by quasi-in situ HRTEM microscopy.

by ex situ TEM. A representative HRTEM image and the particle size distribution of the postreaction Pd/Ga₂O₃ catalyst are shown in Fig. 5a and b, respectively. Dramatic nanostructural changes appeared in the material: most of the palladium crystallites became

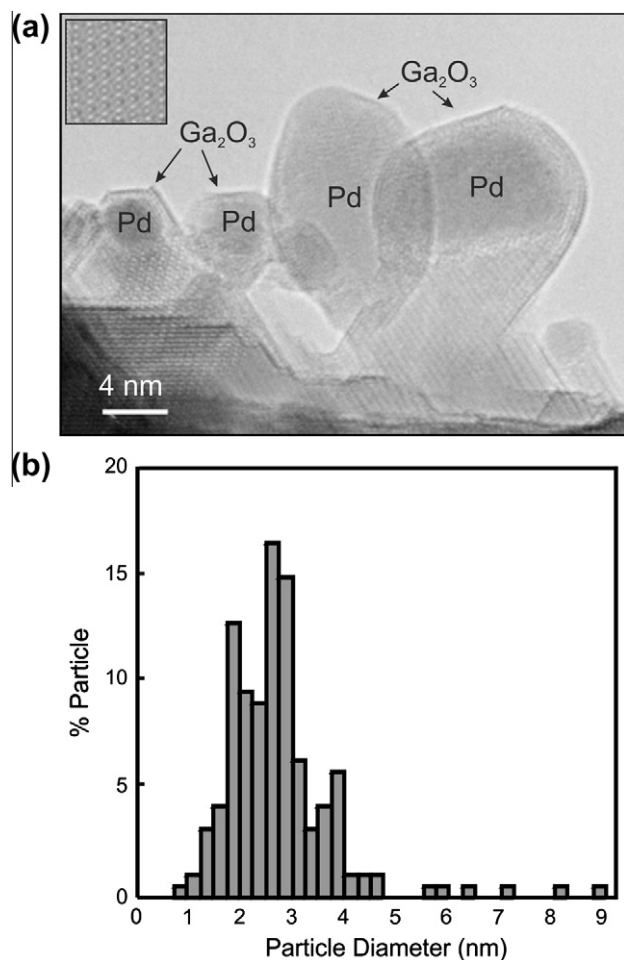


Fig. 5. (a) HRTEM image of the postreaction Pd/β-Ga₂O₃ catalyst (inset: [101] zone axis simulation image of a β-Ga₂O₃ crystal) and (b) metal particle size distribution.

covered by a thin layer that grew on top of the metal crystal planes. A phase simulation of β-Ga₂O₃ along the zone [101] axis has been inserted in the upper left corner of Fig. 5a. It fits perfectly to the phase observed in both the oxide support and the thin layer decorating the Pd particles. Therefore, we could conclude that the gallia phase decorating the Pd particles was crystalline and monoclinic.

It was further noted that the thin layers of the support phase grew epitaxially to the faceted surface planes of the metal particles. In some cases, these metal particles were settled on a stand, or “pedestal,” of the support. It is likely that these stands grew under the original contact surface between the Pd crystallites and the gallia, following the same mechanism that produced the decoration, as analyzed below.

In a recent work [26], HRTEM was used to show that a Ce–Au alloy was formed on Au/CeO₂ under reductive conditions but that, upon reoxidation, ceria segregated onto the metal, encapsulating it with a film of CeO₂. A similar mechanism was also suggested for other supported noble metals, such as platinum [27,28].

The lattice spacing of the encapsulated particles corresponded to metallic Pd. That is, no relaxation (indicative of a bimetallic phase or Pd–Ga alloy) was observed. However, as indicated before, DDP analysis does not allow clear identification of Pd–Ga phases, due to the interference of the oxide layer. Fig. 5b shows a moderate increase in the metal particle sizes to 2.8 nm and a decrease in the dispersion, D_{TEM} (down to 33%), in comparison to the as-prepared (i.e., reduced and passivated) sample. X-ray diffraction patterns of the as-prepared, re-reduced (as-prepared + R523/6 h + air-exposed), and postreaction Pd/Ga₂O₃ catalysts were also taken (spectra not shown), but only the characteristic monoclinic structure of the β-Ga₂O₃ support was registered (i.e., no Pd, Pd–Ga alloy, or PdO diffraction peaks). This result was most likely due to the low metal loading and small particle size of the palladium crystallites.

3.3. In situ Fourier transform infrared characterization

3.3.1. CO adsorption by infrared spectroscopy

The as-prepared Pd/β-Ga₂O₃ catalyst was exposed to a series of reduction steps in pure H₂ (760 Torr, 100 m³ min⁻¹) at increasing temperatures of 423, 523, and 723 K (60 min each time), evacuated at the same temperature for 60 min, and cooled under vacuum to RT. After each reduction treatment, the catalyst was exposed to 10 Torr CO at room temperature for 10 min. The collected spectra are shown in Fig. 6. After the Pd/β-Ga₂O₃ catalyst that was reduced at 423 K was exposed to CO, several absorption bands corresponding to the linear (L = 2092 cm⁻¹), bridged (B = 1975 cm⁻¹), and threefold bridged or hollow (H = 1915 cm⁻¹) forms were observed [29–31]. This spectrum was very similar to the one obtained after the adsorption of CO (10 Torr, RT) on Pd/SiO₂ [32]. After reduction at higher temperatures (523 and 723 K), the spectra clearly showed a progressive loss of intensity of the bridged CO bands (B and H) and a moderate increase in the linear CO signal.

Kovnir et al. [19] reported the characterization of Pd–Ga bimetallic particles using CO chemisorption followed by FTIR. No adsorption of CO in its bridged forms appeared on this Pd–Ga system, and only one sharp band with a maximum at 2047 cm⁻¹, assigned to CO adsorbed on Pd in the on-top position, was observed. This finding was interpreted as being the result of the isolation of Pd atoms on the surface of PdGa, as expected from the bulk crystal structure of the intermetallic compound. The breakdown of the arrangement among adjacent Pd atoms, or the increase in the distance between adjacent Pd atoms, prevented the adsorption of CO in the bridged form. The significant red shift of the CO(L) band was ascribed to a strong electronic modification of Pd in the intermetallic compound, as detected by XPS measurements [19]. Identical results were reported very recently by Haghofer et al. using gallia-supported palladium [22].

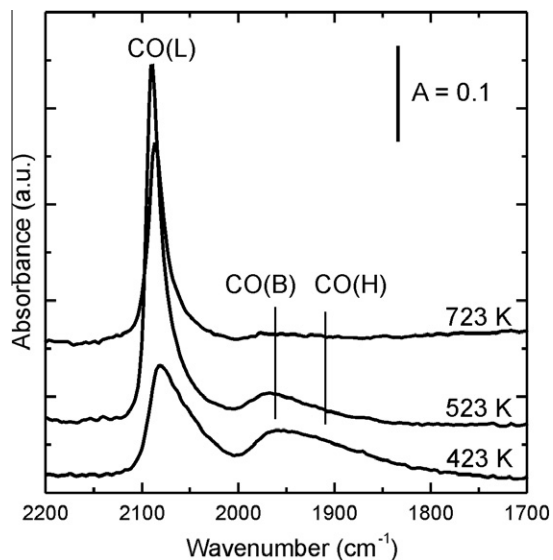


Fig. 6. FTIR spectra after CO adsorption (10 Torr, 300 K, 10 min) over the Pd/ β -Ga₂O₃ catalyst prereduced in situ in pure H₂ (60 min, 100 cm³ min⁻¹) at 423, 523, and 723 K.

We also performed a CO adsorption experiment (pulses), at RT, over the activated catalyst (as-prepared + R523/1 h). The obtained metal dispersion, D_{CO} (calculated using a CO/Pd = 1/1 stoichiometry), was 31%, a value somewhat smaller than the one deduced from TEM size distribution data (41%) (on the reference Pd/SiO₂ catalyst, D_{TEM} and D_{CO} were equal; Table 1). These results also indicated a loss of Pd metal sites at the surface of the particles due to bimetallic particle formation, since CO chemisorption on this material as measured by FTIR—spectra not shown—is irreversible.

3.3.2. CO₂ hydrogenation at RT

The hydrogenation ability of the Pd–Ga bimetallic particles was tested by in situ FTIR spectroscopy after activation of samples of the as-prepared Pd/ β -Ga₂O₃ catalyst. As reported above, palladium catalysts supported on (or promoted with) Ga₂O₃ are able to hydrogenate the (bi)carbonate species bonded to the gallia surface that appear upon adsorption of CO₂, producing formate even at ambient temperature [10]. This test reaction was used here to measure the ability of the metal particles to chemisorb and spillover hydrogen to the support. Briefly, after reduction in pure hydrogen at 523 K for 1 h, the sample wafers were evacuated at the same temperature for 30 min and cooled to RT under vacuum. Then pure CO₂ was flowed (100 cm³ min⁻¹) at room temperature for 15 min, producing (bi)carbonate species on the gallium oxide surface [9]. Next, the flow was changed from pure CO₂ to a H₂/CO₂ = 3 (100 cm³ min⁻¹) mixture. As shown in Fig. 7, complete hydrogenation of the (bi)carbonate surface species to formate (HCOO) was observed in the activated prereduced Pd/Ga₂O₃ catalyst after approximately 5 min on stream at RT (m-HCOO [$\nu_{as}(OCO)$ = 1660 cm⁻¹, $\delta(CH)$ = 1309 cm⁻¹, $\nu_s(OCO)$ = 1272 cm⁻¹], br-HCOO [$\nu_{as}(OCO)$ = 1580 cm⁻¹, $\delta(CH)$ = 1382 cm⁻¹, $\nu_s(OCO)$ = 1362 cm⁻¹] and b-HCOO [$\nu_{as}(OCO)$ = 1600 cm⁻¹]) [10].

The postreaction catalyst, which predominantly contained fully encapsulated metal particles, was also tested for the hydrogenation of carbonates at RT. A wafer of this material was reduced just at 343 K, to avoid as much as possible the rupture (re-reduction) of the gallia-layer-decorated Pd crystallites. As has already been established, H₂ treatment at such a temperature is sufficient to reduce supported palladium particles to the metallic state. The experimental results showed almost no hydrogenation of these

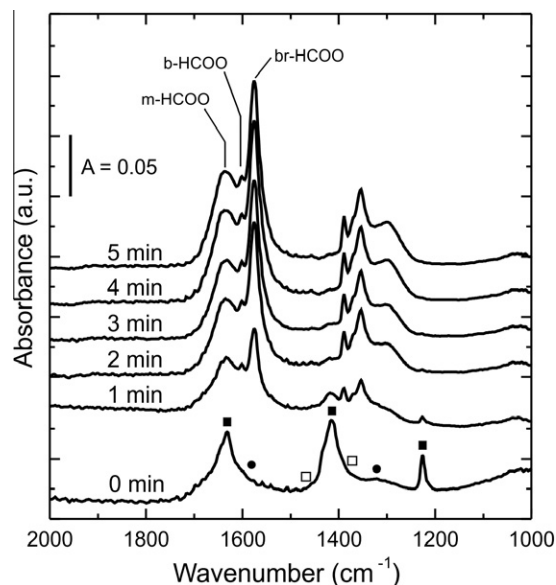


Fig. 7. Hydrogenation of surface (bi)carbonate groups bound to the gallia surface to formate species over Pd/ β -Ga₂O₃ prereduced at 423 K after switching from a pure CO₂ stream (100 cm³/min) to a H₂/CO₂ = 3 mixture (100 cm³/min). Total pressure = 0.1 MPa. Solid squares: bicarbonates; solid circles: bidentate carbonates; open squares: polydentate/monodentate carbonates.

surface carbonates on the postreaction catalyst (spectra not shown). This result was expected due to the inhibition of hydrogen dissociation at RT over the gallia-decorated metal particles.

3.4. High-pressure in situ reaction of H₂ and CO₂ followed by Fourier transform infrared

An FTIR study of CO₂ hydrogenation on the activated Pd/Ga₂O₃ catalyst (as-prepared + R523/1 h) was carried out at 0.7 MPa. Before the reaction test was performed, the catalyst was reduced in the reactor cell at 523 K under H₂ flow (100 cm³ min⁻¹, 0.1 MPa). Then the cell was purged with He (100 cm³ min⁻¹, 0.1 MPa) and reference spectra were collected. Next, a H₂/CO₂ mixture (H₂/CO₂ = 3/1) was flowed through the cell at 523 K and 0.7 MPa. Infrared spectra were simultaneously collected every 5 min. Fig. 8a shows the time-resolved infrared spectra collected after switching from pure H₂ to H₂/CO₂ at 0.7 MPa. Almost immediately, hydrogenated surface species bonded to the Ga₂O₃ surface appeared (m-HCOO, br-HCOO, and CH₃O) [10,12], as did linear [CO(L)] and a very weak signal for bridged [CO(B)] bonded carbon monoxide on the Pd sites [32]. The evolution of these surface species is shown in Fig. 8b. The surface concentration of all these species increased during the first 10 min and then reached a steady state after approximately 40 min.

After the gas flow was switched back to pure H₂, with the total pressure kept constant (0.7 MPa), a sharp decrease in m-HCOO and an increase in the CH₃O concentration (Fig. 9a and b) occurred. Meanwhile, the signal intensity of br-HCOO decayed steadily, but no more CH₃O groups were produced after 20 min (the CO₂ partial pressure inside the cell decreased to zero in <5 min—dotted line).

4. Discussion

4.1. Catalyst composition and reactivity

The time evolution of the catalytic activity of the activated Pd/ β -Ga₂O₃ catalyst (as-prepared + R523/1 h) upon its exposure to the stoichiometric H₂/CO₂ mixture (Fig. 1) shows a remarkable

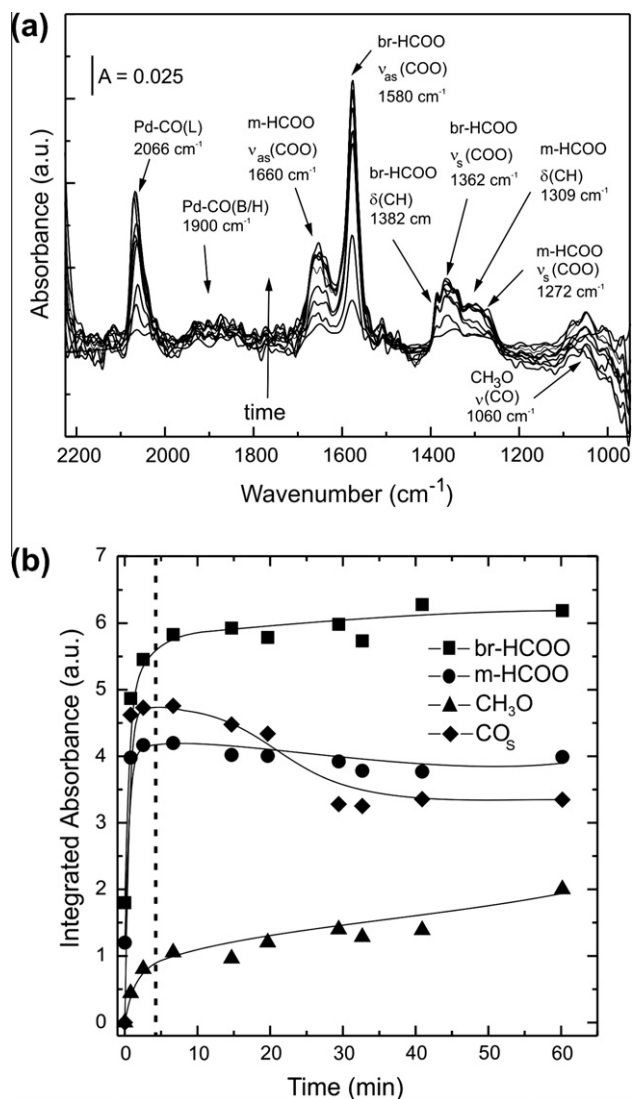


Fig. 8. (a) Time-resolved IR spectra over Pd/ β -Ga₂O₃ at $P = 0.7$ MPa and $T = 523$ K after switching from pure H₂ (100 cm³ min⁻¹) to H₂/CO₂ (molar ratio = 3/1, 140 cm³ min⁻¹). (b) Time evolution of the integrated intensity of the IR bands of the surface species after the switch: br-HCOO [$\nu_{as}(\text{CO}_2) = 1580$ cm⁻¹], m-HCOO [$\nu_{as}(\text{CO}_2) = 1660$ cm⁻¹], CH₃O [$\nu(\text{CO}) = 1060$ cm⁻¹], and CO(L) [$\nu(\text{CO}) = 2066$ cm⁻¹].

change in the selectivity to methanol and CO during the first 3 h, which was entirely absent in the reference Pd/SiO₂ catalyst. Nanostructural and nanochemical analyses by TEM of the catalyst in the as-prepared hydrogen-reduced state at 523 K and the spent catalyst taken from the reactor were also performed. As shown, the as-prepared catalyst possessed predominantly metallic palladium particles on the support, as well as some metal crystallites partially covered by an amorphous layer of gallia. When the catalyst was reduced at 523 K (pure H₂; 6 h) and then studied by TEM without exposure to air, no decorated metal particles were observed. However, the presence of bimetallic Pd–Ga particles was revealed. As mentioned above, the exact composition of these bimetallic Pd–Ga nanoparticles could not be identified by means of its diffraction pattern due to the very close resemblance between pure palladium and bimetallic phases such as Pd₅Ga₂, Pd₅Ga₃, and Pd₂Ga [20]. Conversely, in the case of the air-exposed postreaction catalyst, a remarkable encapsulation of the metal particles by a crystalline layer of β -Ga₂O₃ was observed.

At the surface level, FTIR spectroscopy of adsorbed CO revealed that upon submission of the catalyst to successive reductions with hydrogen at increasing temperature, carbon monoxide no longer

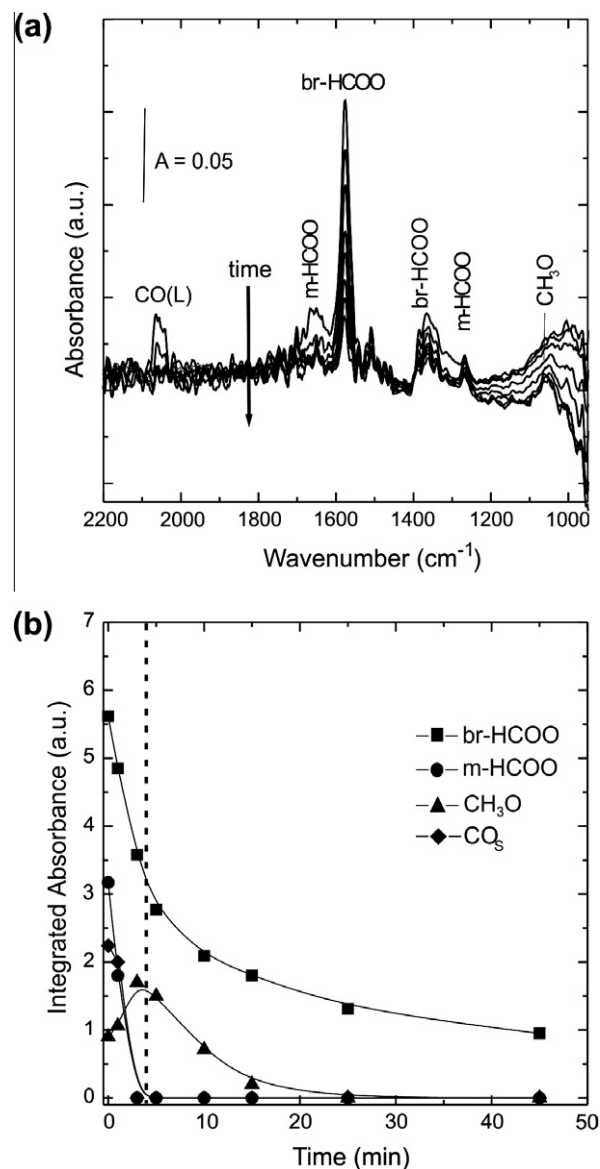


Fig. 9. (a) Time-resolved IR spectra over Pd/ β -Ga₂O₃ at $P = 0.7$ MPa and $T = 523$ K after switching from H₂/CO₂ (molar ratio = 3/1, 140 cm³ min⁻¹) to pure H₂ (100 cm³ min⁻¹). (b) Time evolution of the integrated intensity of the IR bands of the surface species after the switch: br-HCOO [$\nu_{as}(\text{CO}_2) = 1580$ cm⁻¹], m-HCOO [$\nu_{as}(\text{CO}_2) = 1660$ cm⁻¹], CH₃O [$\nu(\text{CO}) = 1060$ cm⁻¹], and CO(L) [$\nu(\text{CO}) = 2066$ cm⁻¹].

chemisorbs in bridged forms, but does so only in the linear or on-top position (Fig. 7). This feature, showing the progressive isolation of the Pd sites, was ascribed to the gradual formation of Pd–Ga bimetallic particles. Similar results were recently reported by Klötzer and coworkers. Using XRD and HRTEM, they showed that Pd–Ga bimetallic particles were produced after reduction pre-treatments at temperatures above 523 K. Furthermore, after the sample was reoxidized, a gallium oxide layer that covered the metal, causing its encapsulation, was also present [20,21].

Contemporary with our work, but in regard to the methanol steam reforming reaction, Haghofer et al. [22] studied in depth a Pd (5 wt.)/Ga₂O₃ catalyst. By in situ XRD, they found that bulk Pd₂Ga and Pd–Ga bimetals were formed after the material was reduced at 673 and 773 K, respectively, and they appeared to be stable in air at room temperature. However, they also reported (as revealed via FTIR by CO chemisorption) that the surface composition of these bimetallic particles significantly changed either after exposure of the catalyst to synthetic air at 303 K due to the

formation of Ga₂O₃ patches or by contact with CO due to restructuring. Nevertheless, under methanol steam reforming conditions (using in operando FTIR), part of the particles consisted of metallic Pd. This result contrasted with what had been observed after hydrogen reduction and CO adsorption, thus indicating that partial decomposition of the bimetallic phase had occurred. Therefore, we could conclude that an analogous process occurred with our Pd/ β -Ga₂O₃ catalyst: (some phase of) Pd–Ga bimetallic particles as formed after the activation of the catalyst at 723 K in 2% H₂, which then (partially, or superficially,) decomposed during the passivation treatment prior to shelving the as-prepared stock material.

Inside the plug-flow microreactor, the re-reduction of the as-prepared catalyst at 523 K for 60 min began to form a Pd–Ga alloy, but certainly the remarkable *initial* selectivity to CO, instead of to methanol, was indicative of Pd–Pd domains on the surface of the metal crystallites. It is likely that during the CO₂ hydrogenation reaction, intermetallic Pd–Ga had already formed and continued incorporating Ga⁰, thus enriching the Pd–Ga alloy. It is also possible that the presence of the produced CO restructured the surface of the nanoparticles during the reaction to bring about both the observable changes in catalyst selectivity during the first 3 h on stream and the steady-state selectivity.

The Pd–Ga bimetallic phase was decomposed upon exposure of the material to oxidizing conditions. Seemingly, gallium can segregate to the surface of the particles and further oxidize after the passivation and removal of the catalyst from the reactor, thereby producing the gallia-encapsulated Pd crystallites shown in the HRTEM micrographs of Figs. 3 and 4.

4.2. Role of Pd–Ga bimetallic particles in the reaction mechanism

As mentioned earlier, the reaction pathway for the hydrogenation of CO₂ to methanol over this same Pd/Ga₂O₃ catalyst was previously explored [10]. Based on detailed and systematic spectroscopic identification of the surface intermediates, the following reaction pathway was proposed: (bi)carbonates, generated by CO₂ adsorption on surface sites of the gallium oxide, are hydrogenated successively to formate(s), methylenebisoxo and methoxy species, and then to methanol. Atomic hydrogen is provided by the supported metal Pd crystallites through H₂ dissociation on the metal, generating active H_s species that spill over onto the support, thereby hydrogenating the carbonaceous intermediates bonded to the gallia surface.

The results presented here also support the bifunctional model, because the hydrogenation of (bi)carbonate species to formate in the as-prepared + R523/1 h catalyst readily proceeds at room temperature, through the spillover of H_s from the bimetallic particles to the support (Figs. 7 and 8).

In addition to carbon oxide(s) hydrogenation and methanol steam reforming [15,16,20–22], Pd–Ga intermetallic catalysts have also been investigated for the selective (or partial) hydrogenation of acetylene in the recent years [17]. These catalysts, particularly bulk Pd–Ga and Pd₃Ga₇, exhibited remarkable selectivity for the partial hydrogenation of C₂H₂ in the presence of a large excess of ethylene. The high selectivity was assigned to the isolation of the palladium active sites due to the crystallographic structure of said Pd–Ga intermetallic compounds, which resulted in a geometric effect and led to weakly π -bonded acetylene molecules on top of the isolated Pd atoms. In addition, an electronic effect resulting in the modification of the adsorption and desorption properties of the acetylene and a kinetic effect due to the decreased availability of hydrogen because of the absence of Pd hydrides were proposed as well [17]. Nevertheless, the Pd–Ga intermetallic compounds were still able to activate and dissociate H₂ to selectively hydrogenate the weakly adsorbed acetylene species.

Our research indicated that bimetallic Pd–Ga particles were responsible for the hydrogenation ability of our catalyst as well. The experimental results indicated that bimetallic surfaces were indeed present from the beginning of the hydrogenation of CO₂ to methanol on this Pd/Ga₂O₃ catalyst. Furthermore, the presence of bimetallic surfaces could be indirectly observed through FTIR study of CO₂ hydrogenation at 0.7 MPa and 523 K. As shown in Fig. 9 and 10, extremely weak signals (almost indistinguishable from the background) from bridged CO were registered, but strongly bound linear CO was clearly observable. It is worth noting that CO(B) species exhibit higher adsorption energy than linear species on palladium; therefore, on supported Pd catalysts (e.g., Pd/SiO₂), they remain adsorbed at temperatures much higher than 523 K [26]. Hence, the presence of these Pd–Ga bimetallic particles during the H₂/CO₂ reaction could be inferred from in situ FTIR at 0.7 MPa (Fig. 8). At this pressure, the activated catalyst was able to hydrogenate CO₂ to methanol (Table 1).

Furthermore, these in situ results suggest that methoxy/methanol formation from H₂/CO₂ took place as a consequence of m-HCOO hydrogenation, while br-HCOO behaved more like a spectator, or laggard reaction intermediate. The key role of monodentate formate bound to Ga₂O₃ in methanol synthesis has already been demonstrated on the basis of theoretical and experimental results [33].

The new experimental evidence reported here allowed reinterpretation of the dramatic change in selectivity of the Pd/Ga₂O₃ catalyst at the beginning of the H₂/CO₂ reaction within the framework of our postulated reaction mechanism. Thus, if the selectivity toward methanol increased as a result of the progressive formation of a Pd–Ga alloy under the (reductive) reaction conditions, said increase in CH₃OH production rate in detriment of CO production could certainly be a consequence of the lower activity of the (newly formed) Pd–Ga bimetallic particles to decompose methanol to H₂ and CO retaining the hydrogen dissociation (metallic) function. This assertion is supported by recent work in the methanol steam reforming reaction [15,16,20–22]). Therefore, methanol is produced via a bifunctional mechanism whereby H₂ can still be dissociated over the Pd–Ga bimetallic particles and spillover to the gallia sites where CO₂ is hydrogenated stepwise.

Therefore, because the “dynamic equilibrium between bimetallic Pd–Ga formation by hydrogen and decomposition of the alloy (at the superficial level) by CO occurs during the reaction” [22], the high partial pressure of H₂ (ca. 2 MPa) during the CO₂/H₂ reaction could keep (or even increase the surface concentration of Ga⁰ on the metal particles). This behavior would counteract the decomposition of the alloy by the produced CO. This in turn should decrease methanol decomposition, which is a property of pure Pd arrays.

It must be recalled that the decrease in CO production with time on the Pd/ β -Ga₂O₃ catalyst was almost threefold larger than the increase in methanol production (Fig. 1). At this point, we can only dwell on along the following line of thought: carbon monoxide production via the reverse water–gas shift reaction (CO₂ + H₂ \leftrightarrow CO + H₂O) proceeds efficiently on Pd particles, as observed in the case of Pd/SiO₂ (Fig. 1). Yet, the progressive on stream reformation of the Pd–Ga bimetallic in the (as-prepared + 523/1 h) Pd/ β -Ga₂O₃ catalyst effectively inhibited the RWGS reaction on the metallic phase, and the material still remained efficiently active for the provision of atomic hydrogen to the carbonaceous species chemisorbed onto the support.

5. Conclusions

A progressive change in selectivity during the CO₂ reaction with H₂, increasing the yield of methanol at the expense of the undesired CO, was observed under typical process conditions. The formation

of Pd–Ga bimetallic particles was identified by means of a combination of quasi-in situ transmission electron microscopy techniques and CO adsorption experiments. The role of these Ga–Pd bimetallic particles in the reaction mechanism of methanol synthesis was the same as that of pure Pd: to dissociate and spill over H to the gallia sites, where CO₂ was stepwise hydrogenated to methanol. Additionally, the decrease in CO production, by inhibition of the methanol decomposition and/or reverse water–gas shift reaction, on the bimetallic phase could be inferred. Gallia encapsulation of the Pd particles constituted an ex situ artifact.

Acknowledgments

Financial support from the Agencia Nacional para la Promoción de la Ciencia y Tecnología of Argentina (ANPCyT) and the Agencia Española de Cooperación Internacional of Spain (AEI) is gratefully acknowledged. S.E.C., M.A.B., and A.L.B. thank the Consejo Nacional de Investigaciones Científicas y Técnicas (CONICET) and Universidad Nacional del Litoral (UNL) for their continued support.

References

- [1] L. Fan, K. Fujimoto, *J. Catal.* 150 (1994) 217.
- [2] W.X. Pan, R. Cao, D.L. Roberts, G.L. Griffin, *J. Catal.* 114 (1988) 440.
- [3] G.C. Chinchén, K.C. Waugh, D.A. Wham, *Appl. Catal.* 25 (1986) 101.
- [4] T. Fujitani, M. Saito, Y. Kanai, Y. Watanabe, J. Nakamura, T. Uchijima, *Appl. Catal. A* 125 (1995) L199.
- [5] T. Fujitani, I. Nakamura, *Bull. Chem. Soc. Jpn.* 75 (2002) 1393.
- [6] A.L. Bonivardi, D.L. Chivassa, C.A. Querini, M.A. Baltanás, *Stud. Surf. Sci. Catal.* 130D (2000) 3747.
- [7] S.E. Collins, M.A. Baltanás, J.L. García-Fierro, A.L. Bonivardi, *J. Catal.* 211 (2002) 252.
- [8] S.E. Collins, M.A. Baltanás, A.L. Bonivardi, *Langmuir* 21 (2005) 962.
- [9] S.E. Collins, M.A. Baltanás, A.L. Bonivardi, *J. Phys. Chem. B* 110 (2006) 5498.
- [10] S.E. Collins, M.A. Baltanás, A.L. Bonivardi, *J. Catal.* 226 (2004) 410.
- [11] S.E. Collins, M.A. Baltanás, A.L. Bonivardi, *Appl. Catal. A* 295 (2005) 126.
- [12] S.E. Collins, L.E. Briand, L.A. Gambaro, M.A. Baltanás, A.L. Bonivardi, *J. Phys. Chem. C* 112 (2008) 14988.
- [13] S.E. Collins, D.L. Chivassa, A.L. Bonivardi, M.A. Baltanás, *Catal. Lett.* 103 (2005) 83.
- [14] D.L. Chivassa, S.E. Collins, A.L. Bonivardi, M.A. Baltanás, *Chem. Eng. J.* 150 (2009) 204.
- [15] N. Iwasa, T. Mayanagi, N. Ogawa, K. Sakata, N. Takezawa, *Catal. Lett.* 54 (1998) 119.
- [16] N. Iwasa, T. Mayanagi, W. Nomura, M. Arai, N. Takezawa, *Appl. Catal. A* 248 (2003) 153.
- [17] J. Osswald, K. Kovnir, M. Armbruster, R. Giedigkeit, R.E. Jentoft, U. Wilda, Y. Grinb, R. Schlögl, *J. Catal.* 258 (2008) 219.
- [18] M. Armbrüster, K. Kovnir, M. Behrens, D. Teschner, Y. Grin, R. Schlögl, *J. Am. Chem. Soc.* 132 (2010) 14745.
- [19] K. Kovnir, M. Armbruster, D. Teschner, T.V. Venkov, L. Szentmiklosi, F.C. Jentoft, A. Knop-Gericke, Yu. Grin, R. Schlögl, *Surf. Sci.* 603 (2009) 1784.
- [20] S. Penner, H. Lorenz, W. Jochum, M. Stöger-Pollach, D. Wang, C. Rameshan, B. Klötzer, *Appl. Catal. A* 358 (2009) 193.
- [21] H. Lorenz, S. Penner, W. Jochum, C. Rameshan, B. Klötzer, *Appl. Catal. A* 358 (2009) 203.
- [22] A. Haghofner, K. Föttinger, F. Girdsies, D. Teschner, A. Knop-Gerike, R. Schlögl, G. Rupprechter, *J. Catal.* 286 (2011) 13.
- [23] S.E. Collins, M.A. Baltanás, A.L. Bonivardi, C. Mira, J.J. Calvino, S. Bernal, 14th International Congress in Catalysis, June 15, 2008, Seoul, Korea.
- [24] C.S. Fung, C.A. Querini, *J. Catal.* 138 (1992) 240.
- [25] K. Khalaff, K. Schubert, *J. Less-Common Met.* 37 (1974) 129.
- [26] T. Akita, M. Okumura, K. Tanaka, M. Kohyama, M. Haruta, *Catal. Today* 117 (2006) 62.
- [27] S. Bernal, F.J. Botana, J.J. Calvino, G.A. Cifredo, J.A. Pérez-Omil, J.M. Pintado, *Catal. Today* 23 (1995) 219.
- [28] S. Bernal, J.J. Calvino, M.A. Cauqui, J.M. Gatica, C. Larese, J.A. Pérez Omil, J.M. Pintado, *Catal. Today* 50 (1999) 175.
- [29] E. Ozensoy, D.W. Goodman, *Phys. Chem. Chem. Phys.* 6 (2004) 3765.
- [30] T. Lear, R. Marshall, J.A. López-Sánchez, S.D. Jackson, T.M. Klapötke, M. Bräumer, G. Rupprechter, H.J. Freund, D. Lennon, *J. Chem. Phys.* 123 (2005) 174706.
- [31] F.M. Hoffmann, *Surf. Sci. Rep.* 3 (1983) 1.
- [32] S.E. Collins, M.A. Baltanás, A.L. Bonivardi, *J. Mol. Catal. A* 281 (2008) 73.
- [33] M. Calatayud, S.E. Collins, M.A. Baltanás, A.L. Bonivardi, *Phys. Chem. Chem. Phys.* 11 (2009) 1397.